Statistical Analysis and Detection of Spread-F and foF2 values using Digisonde and VIPIR instruments

Preeti Bhaneja (Preeti.Bhaneja@nasa.gov), Terry Bullett, Jeff Klenzing

ABSTRACT

Statistical studies of spread F for low, mid and high latitude regions using digisonde data. Various algorithms have been written to process the raw data and determine spread F by using edge detection and pattern recognition techniques along with foF2 and hmF2 values. Findings based on work carried out to date include:

•Differentiating different types of spread F at low and high latitudes.
•Observation of particle precipitation at high latitudes.
•Determination of seasonal and solar cycle variation patterns.
•Correlation between digisonde, COSMIC-1 satellite data and SAMI and IRI models values to check for validity of data.

INTRODUCTION

Density irregularities in the ionosphere are often observed as a spread pattern in data from radio sounding techniques such as digisondes referred to as Spread F. Spread F is observed at equatorial (ESF), mid (MSF) and high (HSF) latitude regions; all have different instability mechanisms due to the angle of the magnetic field relative to the ionospheric plasma layer.

Ionospheric F region is known to exhibit anomalies and irregularities during both day and night time. Various anomalies have been observed in the ionospheric F2 region as observed in the critical frequency and the electron density values. Ionospheric irregularities are temporal and spatial variations of the electron density lasting from a few minutes to a several hours. Gravity waves are considered to be a seeding mechanism creating density perturbations in the ionosphere leading to spread conditions [*Rishbeth*, 2006]. Atmospheric buoyancy waves, also referred as gravity waves are generated from a variety of sources, including thunderstorms [*Lay et al*., 2015] and auroral disturbances [*Nygren et al*., 2015].

Spread-F is mostly a night-time phenomenon at low and midlatitudes except at high latitudes where it is observed at all times. The irregularities are observed on the ionograms which are plots of frequency vs. height obtained by reflections of the transmitted signal into the ionosphere when they match the plasma frequency [*Bhaneja et al*., 2018, 2009]. For equatorial spread F, the various irregularities or spread patterns may be associated with multiple types of plasma structures, such as plumes, patches, bubbles, and blobs [*Aarons*, 2001]. High latitude spread F is observed as various types including forking, spur and Es [*Penndorf*, 1962].

The data in O-Mode trace is used to generate ionograms for identifying spread F. Ionograms obtained during spread F events show thickness or spread in the F region trace that is significantly greater than that obtained for a normal ionosphere. ***Figure 2*** shows ionograms indicating different conditions of the ionosphere. **Top figure**: 2(a) indicates a quiet ionosphere, represented by a single trace. 2(b), (c) and (d) show ionograms with thick traces which implies strong spread conditions. **Bottom figure**: spread F events for high latitude. 1st column shows the Es events due to particle precipitation; 2nd column shows forked ionograms; 3rd columns shows intense spread with spur. The spread observed on the ionograms can be classified as range or frequency spread. **Range spread** (RS) refers to a condition in which there are multiple range echoes at a particular frequency. **Frequency spread** (FS) refers to the case in which multiple critical frequencies appear at fixed altitudes.

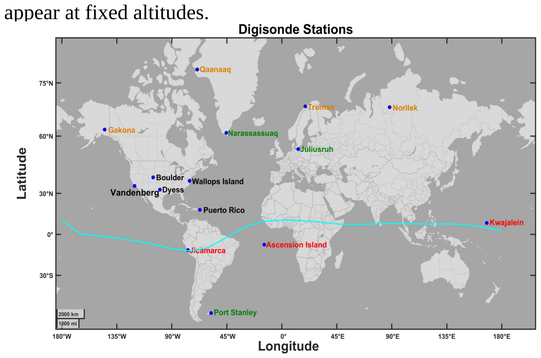

FIGURE 1 –Digisonde stations used in this study. Low latitude sites are in red; mid latitude sites are in black; high latitude sites are in orange. Stations in green are for future study.

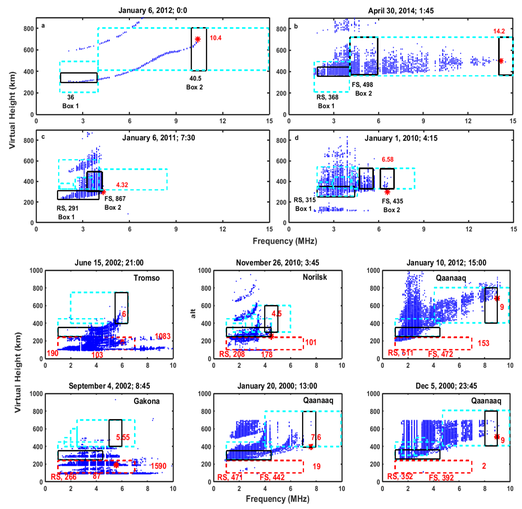

FIGURE 2 – Top figure: a) An ionogram showing a quiet event. Different kinds of Spread F events for low and mid latitudes; b) Range Spread; c) Range and Frequency Spread; d) Spread in a form of a big blob. Bottom figure: various spread F events for high latitude. 1st column (a) & (d) shows the Es events due to particle precipitation. 2nd column (b) & (e) shows the forked ionograms. 3rd column (c) & (f) shows the intense spread with spur. The blue dotted lines are the boundary boxes, and the solid black line box is the box selected by the algorithm for determining Range (RS, Box 1) and Frequency (FS, Box 2) spread F and foF2 for an individual ionogram. The corresponding numbers with RS and FS are the pixel counts in each box which determine the spread F. The red star and the corresponding number is the foF2 value determined for the individual ionogram. The red dotted box is for determining the Es and the corresponding number is the Es pixel count.

DATA PRESENTATION

The dataset is comprised of ionograms at 15 minute intervals. The focus of this study is to determine statistics of spread F events and detect foF2 values. The following ***Figures*** illustrate these findings.

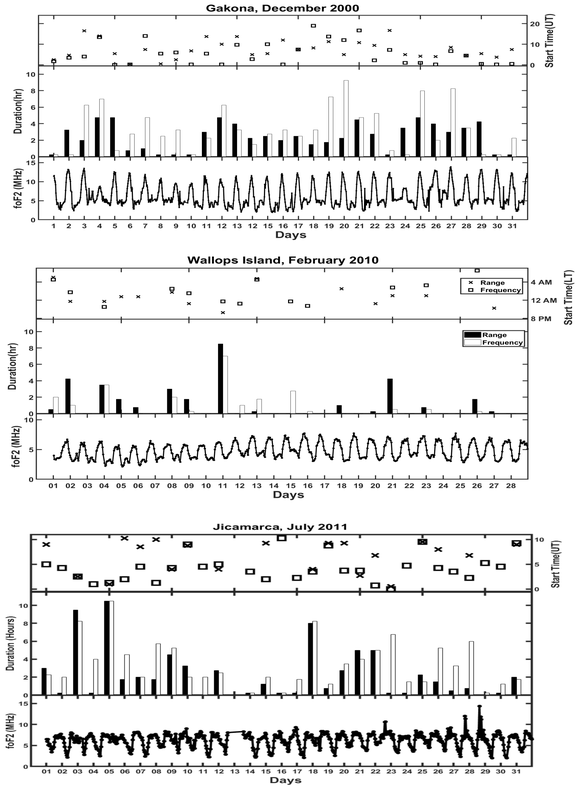

FIGURE 3 –Monthly occurrence plot for Gakona, Wallops Island and Jicamarca showing range and frequency spread F onset time and duration along with the foF2 values. For Wallops, VIPIR data has been used for foF2 values.

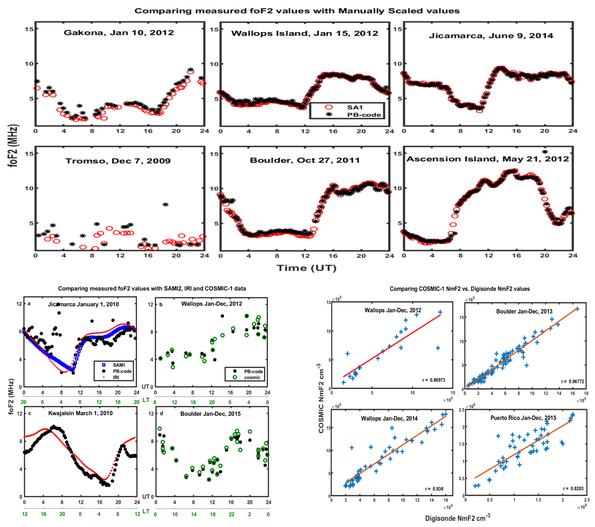

FIGURE 4 – Top figure: Comparison of foF2 from the algorithm developed (PB-code) with manually scaled values (SA1) obtained using SAO Explorer. The 1st column is high latitude stations, 2nd column is mid latitude stations and 3rd column is low latitude stations. Bottom figure: Left Side: Comparison of PB-code detected foF2 with COSMIC-1, SAMI and IRI values. Right Side: Plot showing the COSMIC-1 NmF2 versus the Digisonde NmF2 (PB-code) values for different sites. The regression coefficient is quite high for all the plots and the values appear to be in good agreement.

Figures 5 & 6 show the solar and seasonal cycle variations of high, mid and low latitude regions for the various sites shown in the map in **Figure 1**. The red line in **Figure 6** is the angle between the dusk terminator and local magnetic field. More spread F during minimum angle indicates that efficient electric field mapping between conjugate hemispheres is important for the occurrence of spread F.

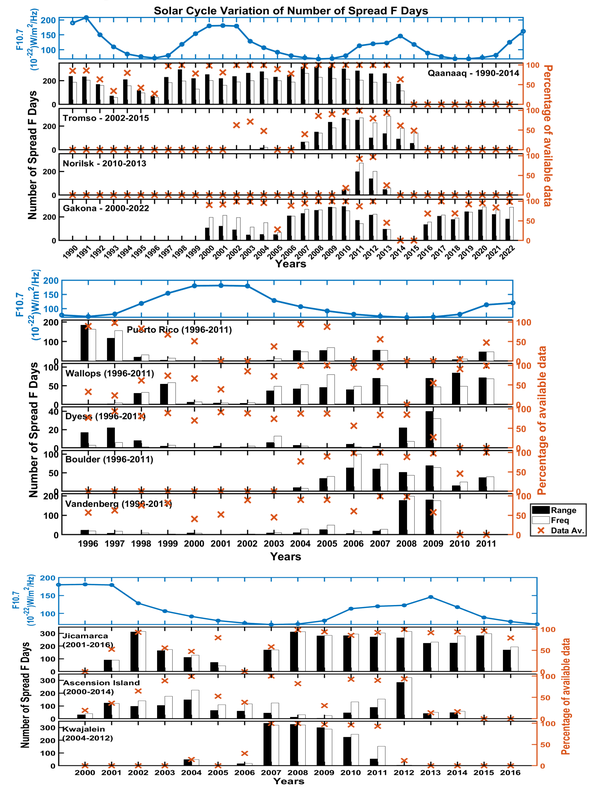

FIGURE 5 –Plots show the solar cycle variation of spread F for high latitude sites; Qaanaaq, Tromso and Norilsk; midlatitude sites; Wallops Island, Puerto Rico, Dyess and Vandenberg and Boulder; low latitude sites; Jicamarca, Ascension Island, and Kwajalein. The left side shows the number of spread F days for range (black bars) and frequency (white bars) spread F and the right side shows the percentage of available data (red crosses). The blue line in top panel is the solar flux.

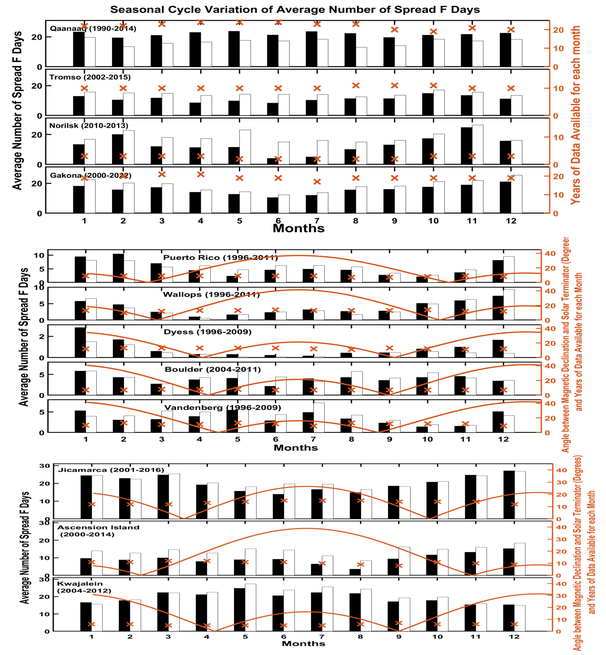

FIGURE 6 – Plot shows the seasonal cycle variation for the sites for the available data. The left-hand side shows the average number of spread days. The right-hand side shows the months of data available (red crosses) and the angle between the declination and the terminator (red line). The black bars represent range spread F while white bars represent frequency spread F.

DISCUSSION

It is evident from ***Figure 4*** that the algorithm detects fairly accurate values of foF2 as shown for different stations with data compared with manually scaled values and also validated by COSMIC-1 satellite measured values and IRI and SAMI model values. NmF2 derived from digisonde data using foF2(MHz)=8.9*sqrt(N(1/cm^-3)), is compared with NmF2 obtained from COSMIC-1 satellite shows regression coefficient higher than 0.87. ***Figure 5*** shows solar cycle variation. MSF occurrence rate and duration is higher during solar min than during solar max for all five stations. Equatorial and high latitude Spread F doesn't have any particular solar cycle variation for the sites. An interesting observation evident is that almost all stations experience more range spread F events during solar min, and more frequency spread F events during solar max. ***Figure 6*** shows seasonal variation. All the stations show different seasonal variations, presumably due to their varying longitudes, declinations, or localized forcing from lower altitude sources. The observations are summarized in **Table 1**. An interesting observation is that places located at negative declination tend to have most spread F conditions during fall and winter seasons while places at positive declination have most spread F during spring and summer seasons.

Stations	Latitude	Longitude	Declination	Season with max MSF	Season with min MSF
Qaanaaq	77.46°	69.22° W	-41.32°	Winter Solstice	Summer (less duration)
Tromso	69.6°	19.2° E	10.49°	Winter Solstice	Summer (less duration)
Norilsk	69.35°	88.19° E	17.25°	Winter Solstice	Summer (less duration)
Gakona	62.38°	145 W°	16.69°	Winter Solstice	Summer (less duration)
Puerto Rico	18.5	67.1	-14°	Winter solstice	Spring equinox, Vernal equinox
Wallops Island	37.95°	75.5°	-11°	Vernal equi., winter sols.	Spring equinox, Summer
Dyess, TX	32.4°	99.8°	6.9°	Winter solstice	Spring, Summer, Vernal Equi.
Boulder, CO	40°	105.3°	10°	Early summer, autumn equi.	Spring Equinox, Winter
Vandenberg, CA	34.8°	120.5°	13°	Summer & winter solstice	Fall
Jicamarca, Peru	12°S	76.8°W	-2.5°	Fall and winter	Spring and Summer
Ascension Is	7.9 S	14.4W	-15.09	Fall and December	Summer
Kwajalein	8.71°N	167.7° E	7.5°	Spring and summer	Fall and winter

WORKS CITED

1. Aarons, J., *Space Science Reviews*, 63, pp. 209-243, 1993.
2. Bhaneja, P., et al., Statistical Analysis of Midlatitude Spread F using Multi-Station Digisonde Observations, *J. Atm.Solar-Terres. Phys*., 167, pp. 146-155, doi.org/10.1016/j.jastp.2017.11.016, 2018.
3. Bhaneja, P., et al., A statistical study of midlatitude spread F at Wallops Island, Virginia, *J. Geophys. Res.*, 114, A04301, doi:10.1029/2008JA013212, 2009.
4. Lay, E. H., at al., *J.Geo.Res.*,10.1002/2015JA021334, 2015.
6. Nygrén, T.,et al., *J. Geophys. Res.*, 120, 3949–3960. doi: 10.1002/2014IA020794, 2015.
7. Penndorf, R., Spread F over the Polar Cap on a Quiet Day,*J. Geophys. Res.*, 67, 12, pp. 4607-4616, 1962.
8.Rishbeth, H., F-region links with the lower atmosphere? *J. Atmos. Solar-Terres. Phys*., 68, 469-478, 2006.